European Review for Medical and Pharmacological Sciences 2021; 25: 1206-1214

HIF-1α repairs degenerative chondrocyte glycolytic metabolism by the transcriptional regulation of Runx2

P. KONG[1], R. CHEN[2], F.-Q. ZOU[1], Y. WANG[2], M.-C. LIU[2], W.-G. WANG[2]

[1]The Affiliated Hospital of Shandong University of Traditional Chinese Medicine, Jinan, China
[2]First Clinical Medical College, Shandong University of Traditional Chinese Medicine, Jinan, China

Abstract. – OBJECTIVE: HIF-1α and Runx2 expression usually increase in chondrocytes (CHs) during osteoarthritis (OA), which involves the changes in glycolytic metabolism. However, the molecular regulation of HIF-1α related to the CHs glycolytic metabolism is still unclear. In this study, we aimed to reveal the mediation of HIF-1α by Runx2 and its effect on the glycolytic metabolism of degenerative CHs.

PATIENTS AND METHODS: The expression of HIF-1α, Runx2, and the degenerative markers of CHs in both natural conditions from the OA patients and IL-1β treated *in vitro* model was analyzed by a Western blot or real-time polymerase chain reaction (RT-PCR). The glycolytic metabolism was determined by the intracellular glucose uptake and adenosine triphosphate (ATP) generation. Transfection of siRNA coding HIF-1α or Runx2 was used to clear the function between HIF-1α and Runx2 in the glycolytic metabolism of degenerated CHs caused by IL-1β. Chromatin immunoprecipitation (ChIP) and Luciferase reporter gene assay were used to verify the Runx2 protein binds to the promoter of HIF-1α and promote its expression.

RESULTS: HIF-1α and Runx2 were increased, and glucose uptake and ATP generation were decreased in the degenerative CHs from both OA and IL-1β conditions. Under the stimulation of IL-1β, Runx2 silencing rejected the upregulation of HIF-1α and further aggravated the glycolytic metabolism. When HIF-1α was silenced, the glycolytic metabolism of CHs was also suppressed. Besides, Runx2 protein could regulate HIF-1α expression in the transcriptional level by binding to its promoter.

CONCLUSIONS: OHIF-1α plays a role in the self-repair of the glycolytic metabolism of degenerative CHs via the transcriptional regulation of Runx2.

Key Words:
Chondrocyte degeneration, HIF-1α, Runx2, Glycolytic metabolism, ATP generation.

Introduction

Osteoarthritis (OA) is a complex arthropathy in which articular cartilage progressively degenerates into the core and is accompanied by synovium, subchondral bone, ligaments, meniscus, adipose tissue, and the entire joint structure changes[1]. Most mammalian cells have undergone a transition of energy metabolism, that is, from a state of static regulation to a state of active metabolism to maintain a balanced state of energy and promote cell survival[2,3]. This metabolic transition also occurs in OA articular cartilage, which affects the metabolic behavior of chondrocytes (CHs)[4].

Articular cartilage is a particular type of connective tissue without blood vessels and a small number of cells. Compared with synovial fluid and plasma, there are far fewer energy substances such as oxygen and glucose available in cartilage[5]. The conversion rate of the outer matrix molecules is relatively low. Therefore, maintaining the delicate balance between cartilage anabolism and catabolism is essential for the long-term integrity and self-repair ability of cartilage tissue[6]. Glucose is a necessary metabolic raw material and structural precursor of cartilage. It is the primary precursor of CHs to synthesize glycosaminoglycans and is very important for the synthesis and degradation of extracellular matrix (ECM). Facilitation of glucose transport is the first step in CH glucose metabolism, which is regulated by hypoxia and proinflammatory cytokines[7,8]. After glucose is transported to CHs, part of it is used to synthesize glycoproteins, partly catabolizes through glycolysis and tricarboxylic acid circulation pathways providing energy for cells, and limited energy is stored in the form of adenosine triphosphate (ATP)[9]. During the pathophysiology of OA, proinflammatory and

Corresponding Author: Weiguo Wang, MD; e-mail: 2015020670@stu.sdnu.edu.cn

pro-catabolic factors increase significantly, catabolism accelerates, and the dynamic balance of cell metabolism is disrupted. Impaired glucose metabolism results in decreased ATP synthesis[10]. Meanwhile, cellular glycolysis level is increased, and anabolic metabolism is accelerated through proliferation and protein synthesis to maintain the dynamic balance of anabolic and catabolic metabolism and meet the energy requirements of CHs[11].

The Hypoxia-inducible factor 1-α (HIF-1α) gene is the primary regulator for cells to adapt to hypoxic stimulation. It plays a vital role in maintaining CH activity and integrity, regulating cartilage formation, energy metabolism, and matrix synthesis[12]. Yudoh et al[13] found that under normoxic and hypoxic conditions, OA CHs lacking HIF-1α cannot maintain energy production and ECM growth, and *in vitro* decomposition stress induces accelerated apoptosis. Therefore, the expression of HIF-1α is closely related to the process of degeneration of cartilage. Cartilage in both regular and OA condition expresses the HIF-1α and its target gene. HIF-1α plays an essential role in maintaining the viability of articular cartilage of OA. The number of HIF-1α positive CHs increases as the severity of OA increases. As a result, CHs may rely on the adaptive function of the HIF-1α gene to maintain ATP levels and ECM production during OA.

Runt-related transcription factor 2 (Runx2), a key transcription factor related to CHs hypertrophy, has already known to be activated in OA[14]. In this study, we show that Runx2 activation in degenerative CHs transcriptional regulates HIF-1α expression by binding to its promoter, which critically controls glucose uptake and ATP generation under pathological conditions. Runx2 deficiency suppresses HIF-1α activation and results in the aggravation of CHs degeneration.

Patients and Methods

Normal and OA Cartilage Source

This study was approved by the Ethics Committee of Shandong University of Traditional Chinese Medicine. Signed written informed consent was obtained from all participants before the course. We collected the knee joint tissue from a total of ten patients (half of which underwent distal femoral amputation caused by osteosarcoma; half underwent total knee replacement caused by OA) in the orthopedics apartment of our hospital. The tissue from femoral amputation was valued without OA history and had no visible degeneration *via* the imaging diagnosis. All patients signed an informed consent form and voluntarily donated joint tissue for scientific research. All the samples were conserved in growth medium immediately after cutting from patients and brought to the laboratory for the following CHs isolation.

CHs Isolation and Cell Culture

The cartilage of the surface layer was separated from the joint and cut into fragments. Then, the sample was digested with a mixture of trypsin and type I collagenase (R&D Systems, Minneapolis, MN, USA) overnight. After centrifuge, cell pellets were re-suspended in Dulbecco's Modified Eagle's Medium (DMEM) (Gibco, Rockville, MD, USA) supplemented with 10% fetal bovine serum (FBS) (Gibco, Rockville, MD, USA) and incubated at 37°C under 5% CO_2. After the cell density reached 70 %, we split the cells and applied them to the following experiments. To induce the CHs degeneration, we cultured the cells with 10 ng/mL IL-1β (Boehringer, Mannheim, Germany) up to three days. Besides, we also transfected the CHs with Small interfering RNA (siRNA) to silence the Runx2 or HIF-1α expression.

Western Blot (WB)

We determined the cellular type II collagen (Col-II), type X collagen (Col-X), Runx2, and HIF-1α protein expression *via* WB analysis. The total protein of CHs was isolated with the radioimmunoprecipitation assay (RIPA) lysis buffer (Beyotime, Shanghai, China). After sodium dodecyl sulfate-polyacrylamide gel electrophoresis (SDS-PAGE), the protein was transferred onto polyvinylidene difluoride (PVDF) membrane (Millipore, Billerica, MA, USA). Membranes were incubated with desired primary antibodies as follows: anti-Coll-II (ab34712, Abcam, Cambridge, UK), anti-Col-X (ab58632, Abcam, Cambridge, UK), anti-Runx2 (ab76956, Abcam, Cambridge, UK), anti-HIF-1α (ab16066, Abcam, Cambridge, UK), anti-β-actin (ab179467, Abcam, Cambridge, UK). After secondary antibody reactions, the protein was detected using the enhanced chemiluminescence (ECL) substrate (Beyotime, Shanghai, China). Band intensities were measured using ImageJ software (NIH, Bethesda, MD, USA).

Glucose Uptake Analysis

CHs were seeded in a 96-well plate at a density of 10^4 per well. After treatment, cells were washed with phosphate-buffered saline (PBS) and changed to serum-free DMEM overnight. Glucose uptake

Table I. Predicted binding sites of Runx2 to HIF-1α promoter.

Predicted sequence	Start	End	Score	PCR primer sequences for ChIP
accaccaat	98	106	9.41	Sense: 5'-ATCTCCGTCCCTCAACCTCT-3'; Anti-sense: 3'-TTCATTGTCTACCCGACTCC-5'
aacgtcaaa	516	524	6.64	Sense: 5'-ATCTGCCTTAGGTTTACAAT-3'; Anti-sense: 3'-ACTTCTTCCTGGTCCTCTTC-5'
ggcgccaaa	1585	1593	9.26	Sense: 5'-CCGCCCCAGGGCCGAGTTTT-3'; Anti-sense: 3'-CCTACCCCGGTGTCTCGTCC-5'

of CHs was measured using the Glucose Uptake Assay Kit (ab136955, Abcam, Cambridge, UK) according to the manufacturer's protocol.

Cellular ATP Detection

After treatments, CHs were harvested and boiled for the cell lysates, and 50 ml of samples/standards were transferred to a white plate. Then, the ATP bioluminescence assay kit (ab113849, Abcam, Cambridge, UK) was added according to the manufacturer's protocol and measured with a luminometer (GloMax Explorer System).

Real-Time Polymerase Chain Reaction (RT-PCR)

We determined the cellular type I collagen (Col-I) and MMP13 mRNA expression *via* RT-PCR analysis. RNA of CHs was extracted using TRIzol reagent (Nippon Gene, Tokyo, Japan) according to the manufacturer's protocol. After reverse-transcription into cDNA, RT-PCR was performed with SYBR Green Master Mix (Invitrogen, Carlsbad, CA, USA). Gene expression was achieved by normalization to GAPDH and calculated using the $2^{-\Delta\Delta Ct}$ method. The primer sequences used for MMP13 is Forward: 5'-ACTGAGAGGCTCCGAGAAATG-3', Reverse: 5'-GAACCCCGCATCTTGGCTT-3'; Col-I is Forward: 5'-GAGGGCCAAGACGAAGACATC-3', Reverse: 5'-CAGATCACGTCATCGCACAAC-3'; GAPDH is Forward: 5'-ACAACTTTGGTATCGTGGAAGG-3', Reverse: 5'-GCCATCACGCCACAGTTTC-3'.

siRNA Transfection

We silenced the Runx2 and HIF-1α gene expression *via* siRNA transfection. Briefly, after seeding culture plate, Opti-MEM (Sigma-Aldrich, St. Louis, MO, USA) and siRNA targeting Runx2 or HIF-1α (Assay ID:115507 or 106498, Thermo Fisher Scientific, Waltham, MA, USA) were added to the Lipo2000 reagent (Invitrogen, Carlsbad, CA, USA). CHs were transfected with the mixture for 24 h and changed the medium.

Chromatin Immunoprecipitation (ChIP) Assay

We selected the 2000-bp upstream promoter region of the HIF-α from the National Center for Biotechnology Information database. We used the JASPAR core database to predict the DNA-binding sites for the Runx2 transcription factor in the HIF-1α promoter. We found seven putative binding sites relative to the transcription start site and chose three of the highest score (Table I) for the following verification using ChIP assay (CST, Danvers, MA, USA). ChIP primers targeting these sites were designed by Primer Premier. The Runx2 (ab236639) antibody was purchased from Abcam (Cambridge, UK). The binding sits of Runx2 to HIF-1α was amplificated by PCR and imaged by agarose gels electrophoresis.

Plasmid Constructs and Luciferase Reporter Gene Assay

WT and mutant HIF-1α DNA promoter sites were synthesized by Generay (Shanghai, China). WT and mutant DNA were cloned into the pGL4.20-basic Luciferase vector to obtain the pGL-WT and pGL-mut plasmids. CHs were transfected with plasmid using Lipofectamine 3000 (Thermo Fisher Scientific, Waltham, MA, USA) according to the manufacturer's protocol. After the transfection of empty vector, Runx2-vector, empty pGL, pGL-plasmid, and pRL (Renilla plasmid), CHs were incubated for 24 h. The cells were lysed, and Luciferase assays were measured and standardized to Renilla Luciferase activity using the Dual-Glo Luciferase Assay System.

Statistical Analysis

Data were analyzed by GraphPad Prism 8 (La Jolla, CA, USA) and expressed as mean ± standard deviation (SD). Differences between the two groups were analyzed using the Student's *t*-test. A comparison between multiple groups was done using one-way ANOVA test followed by Post-Hoc Test (Least Significant Difference). p-value <0.05 shows statistical significance.

Results

Glucose Uptake and ATP Production Decrease in OA CHs

To verify the differential expression of Runx2 and HIF-1α in the CHs of ordinary and OA conditions, we collected the normal and OA cartilage and isolated the CHs. As shown in Figure 1A, OA CHs turned as a hypertrophy-like phenotype, but the normal CHs were rounded and much smaller than the OA condition. As expected, the Col-II protein expression was decreased in the OA CHs, and Col-X, Runx2, and HIF-1α expression were increased compared to the normal (Figure 1B). Besides, the Col-I and MMP13 mRNA expression were also higher in the OA CHs compared to the normal (Figure 1C). To understand the glucose metabolism difference between normal and OA CHs, we tested the glucose uptake and ATP content of both groups. The results indicated that CHs of OA condition took in less glucose and generated less ATP compared to the normal CHs (Figure 1D and E).

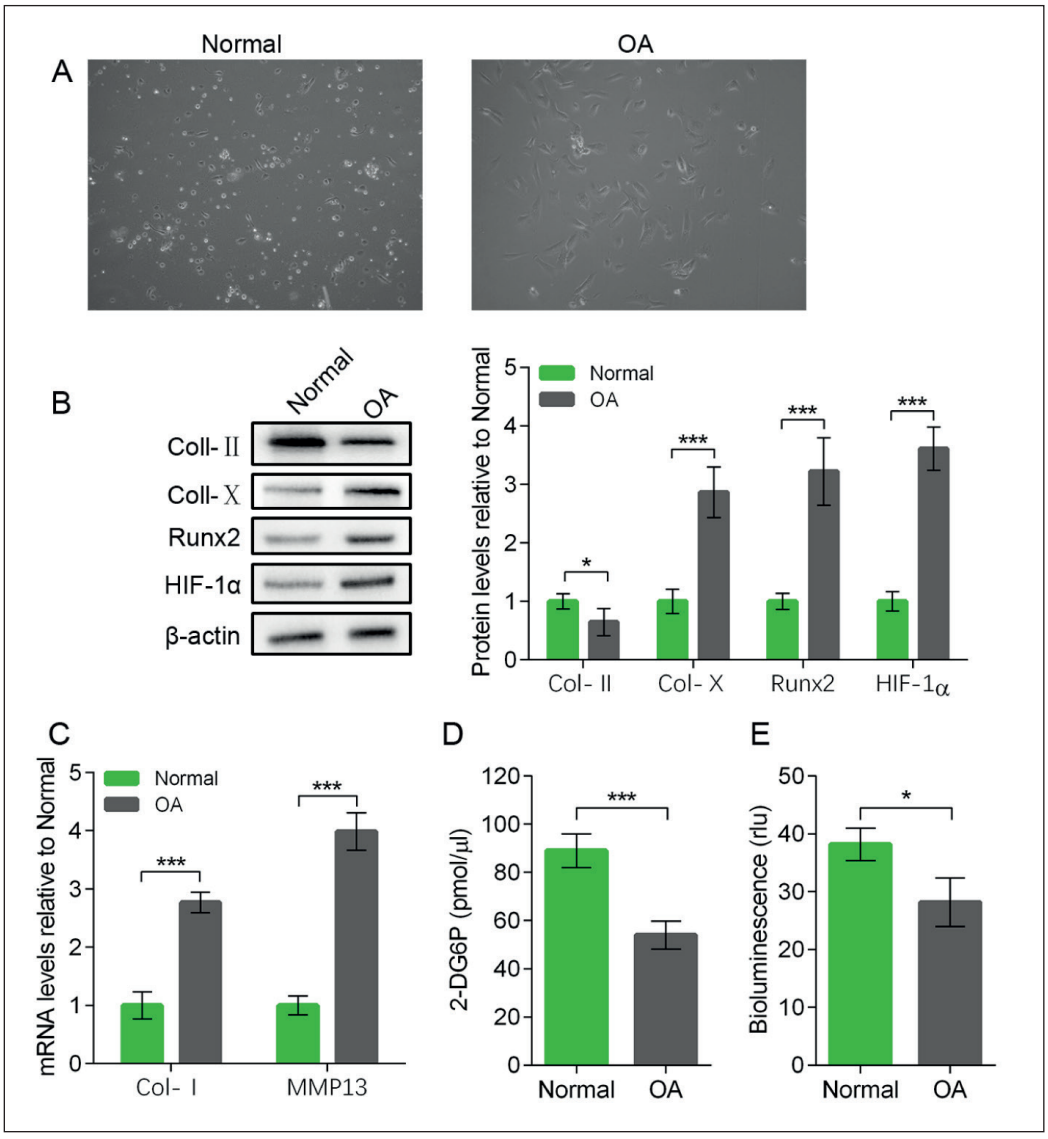

Figure 1. Glucose uptake and ATP production decrease in CHs of OA condition. CHs were isolated from the normal and OA cartilage and seeded to test the glycolytic metabolism. **A**, Images of normal or OA CHs before analysis (magnifications: 200X). **B**, WB analysis for the protein expression of Col-II, Col-X, Runx2, and HIF-1α, and its quantification measured by Image J software. **C**, RT-PCR analysis for Col-I and MMP13 by normalization to GAPDH expression. **D**, Accumulation of 2-deoxy-D-glucose-6-phosphate (2DG6P) in the CHs. E, Relative light units (rlu) of luminescence for ATP bioluminescence assay. Results are expressed as mean ± SD. (*p<0.05, ***p<0.001).

Glucose Uptake and ATP roduction Decrease in IL-1β-Treated CHs In Vitro

We used the IL-1β protein in the culture medium to induce the CHs degeneration *in vitro* and tested the glycolytic metabolism on day 1 and day 3 after stimulation. CHs cultured without IL-1*β* in day 0 were the control group. Compared to the control, the protein expression of the chondrogenic gene Col-II was gradually decreased from day 1 to day 3, and the Col-X, Runx-2, and HIF-1α were steadily increased (Figure 2A). Additionally, the Col-I and MMP13 mRNA expression were also increased from day 1 to day 3 (Figure 2B). Therefore, the IL-1β induced the CHs degeneration and the overexpression of Runx2 and HIF-1α. Like the natural CHs degeneration, we artificially degenerated the CHs *in vitro* and found the glucose uptake and ATP generation were significantly decreased from day 1 to day 3 compared to the control (Figure 2C and D).

Silencing of Runx2 or HIF-1α Aggravates the Decrease of Glucose Uptake and ATP Production in Degenerative CHs

As Catheline et al[15] observed, Runx2 overexpression promotes the hypertrophic progress and the ECM degradation in the OA cartilage, and the upregulated HIF-1α participates in the self-repairment. However, the interaction of Runx2 and HIF-1α in the CH degeneration and glycolytic metabolism is not fully understood. Therefore, we silenced the Runx2 and HIF-1α gene by siRNA transfection and cultured with IL-1β for three days. CHs without siRNA transfection and IL-1β treatment were the control group. As shown in Figure 3A, under the treatment of IL-1β, Runx2 deficient CHs expressed more Col-II and fewer Col-X compared to the normal CHs. However, Runx2 deficient did not affect the HIF-1α expression. Besides, HIF-1α silencing further increased the Col-X expression but did not significantly change the other protein levels compared to the normal cells treated by IL-1β**.** Apart from this,

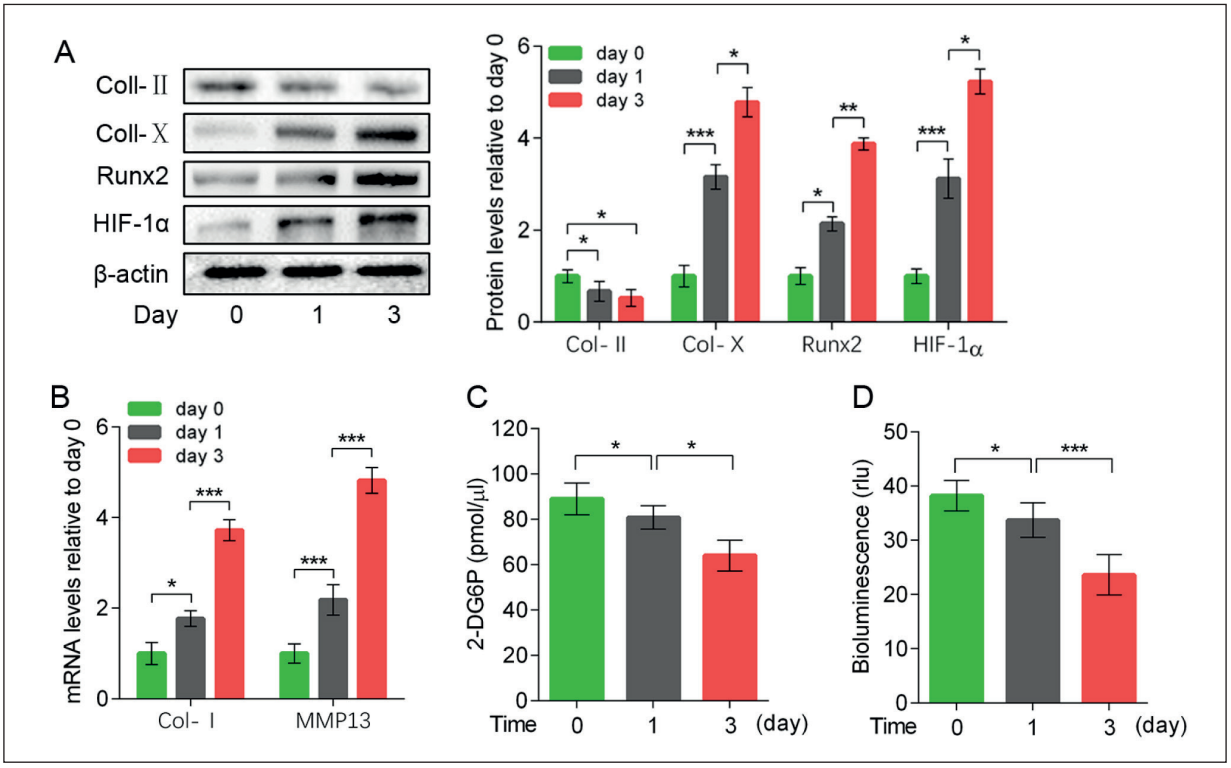

Figure 2. Glucose uptake and ATP production decrease in IL-1β-treated CHs in vitro. CHs isolated from the normal cartilage was cultured with 10 ng/mL IL-1β for 1 day or 3 days. Cells without IL-1β treatment on day 0 were set as control. **A**, WB analysis for the protein expression of Col-II, Col-X, Runx2, and HIF-1α, and its quantification measured by Image J software. **B**, RT-PCR analysis for Col-I and MMP13 by normalization to GAPDH expression. **C**, Accumulation of 2DG6P in the CHs. **D**, Relative light units (rlu) of luminescence for ATP bioluminescence assay. Results are expressed as mean ± SD. (**p*<0.05, ***p*<0.01, ****p*<0.001).

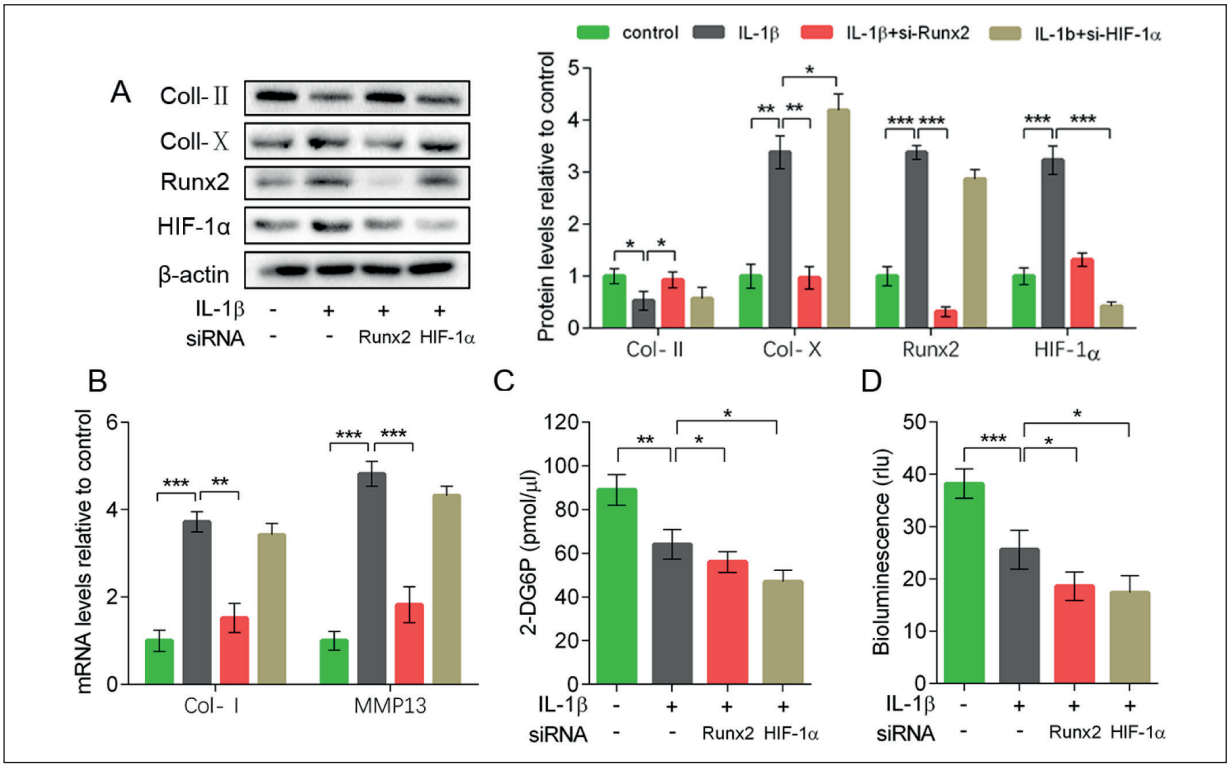

Figure 3. Silencing of Runx2 or HIF-1α aggravates the decrease of glucose uptake and ATP production in degenerative CHs. CHs were transfected with siRNA and subjected to 10 ng/mL IL-1β for 3 days. Cells without transfection and IL-1β treatment were set as control. **A**, WB analysis for the protein expression of Col-II, Col-X, Runx2, and HIF-1α, and its quantification measured by Image J software. **B**, RT-PCR analysis for Col-I and MMP13 by normalization to GAPDH expression. **C**, Accumulation of 2DG6P in the CHs. **D**, Relative light units (rlu) of luminescence for ATP bioluminescence assay. Results are expressed as mean ± SD. (*p<0.05, **p<0.01, ***p<0.001).

Col-I and MMP13 mRNA expression were suppressed when the Runx2 gene was blocked under the treatment of IL-1β (Figure 3B). Therefore, the silencing of Runx2 delayed the IL-1β induced CHs degeneration, and the silencing of HIF-1α somehow aggravated the degradative process. Besides, under the simulation of IL-1β**,** we found the silencing of Runx2 or HIF-1α both further affected the glucose uptake and ATP generation compared to the control group. There was no apparent difference between si-Runx2 and si-HIF-1α group.

Runx2 Binds to the Promoter of HIF-1α and Promotes its Expression

Since the Runx2 and HIF-1α expression were both increased in degenerative CHs, we hypothesized that Runx2 might control the HIF-1α expression. To verify that Runx2 transcriptionally regulated HIF-1α, we identified 3 putative Runx2 binding sites in the HIF-1α promoter region using the Biotechnology Information database (https://www.ncbi.nlm.nih.gov/), which was showed by ChIP assay. As shown in Figure 4A, we defined the three putative binding sites as P1 (ACCACCAAT, from -98bp to – 106bp), P2 (AACGTCAAA from -516bp to -524bp), and P3 (GGCGCCAAA, from -1585bp to -1593bp). After CHs lysis, we pulled down the cellular Runx2 protein by the anti-Runx2 antibody, and we used the CH DNA as a template to amplify the whole HIF-1α promoter segment *via* RT-PCR (lane 1 of Figure 4B). Clear DNA amplification (the sequences for PCR are list in Table I) were examined after immunoprecipitation with beads only (lane 2 of Figure 4B), with irrelevant control IgG (lane 3 of Figure 4B), and with the anti-Runx2 antibody (lane 4 of Figure 4B). The result suggested the P1 and P2 DNA regions were pulled down with the anti-Runx2 antibody, which was the specific binding sites.

Next, we used a double luciferase reporter gene to confirm the Runx2 binding to the HIF-1α promoter and promoting its expression. The WT and mutant binding site of promoter sequences of P1 and P2 were cloned into the pGL plasmids (pGL-wt1/

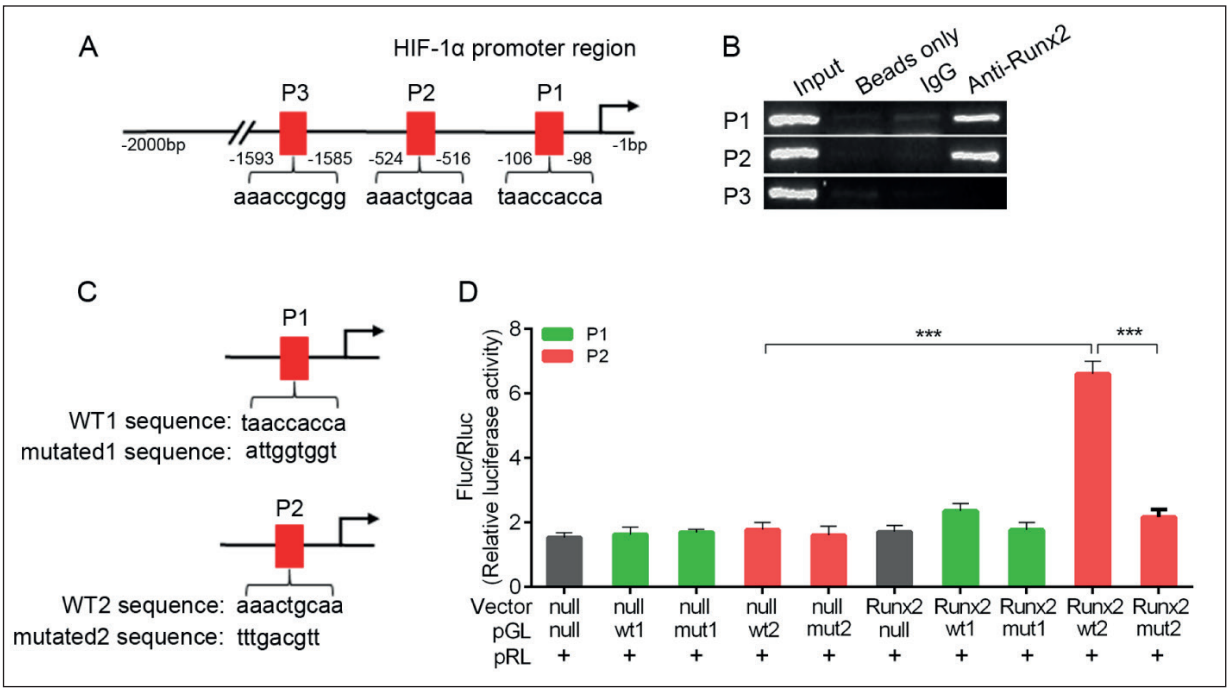

Figure 4. Runx2 binds to the promoter of HIF-1α and promotes its expression. **A**, Three sites in Runx2 predicted to bind the HIF-1α promoter. **B**, P1 and P2 regions of HIF-1α promoter sequences were recovered by PCR from Runx2 immunoprecipitates but not preimmune IgG or beads immunoprecipitates. **C**, Runx2-like elements in the HIF-1α promoter region and the mutated sequence for the pGL4.20 reporter plasmid. **D**, Luciferase activity was driven by the P2 predicted promoter, which was more dramatic following Runx2 treatment, and no significant difference in luciferase activity was observed following Runx2 treatment when P2 sequence was mutated. Results are expressed as mean ± SD. (***p<0.001).

wt2 and pGL-mut1/mut2) and transiently transfected into CHs (Figure 4C). Transfection with empty vector, pGL without the promoter sequence and pRL (vector+pGL+pRL), or with the vector coding Runx2, pGL without the promoter sequence and pRL (Runx2+pGL+pRL) served as the negative controls. The results indicated that transfection with Runx2-vector and pGL-wt2 significantly expressed a higher level of Luciferase activity than in those transfected with empty vector and the pGL-wt2 plasmid (Figure 4D). In contrast, Luciferase activity was significantly lower when the P2 sequence was mutated. Additionally, we did not notice any differences by transfection with the P1 sequence (Figure 4D). Therefore, this finding confirms that P2 is the efficient cite for Runx2 binding to the HIF-1α promoter, which raises a mechanism for Runx2 transcriptionally activating HIF-1α in CHs.

Discussion

In the early stage of OA, the metabolic adaptation of articular cartilage under harmful stimulation conditions is undeniable. CHs dedifferentiate into a hypertrophy-like phenotype and ECM degrades, which is characterized by decreased synthesis of Col-II and newly synthesized Col-I and Col-X, accompanied by the activation of matrix-degrading enzymes such as MMP13. CHs try to repair damaged cell activity and ECM through adaptive changes in metabolism[16]. With the development of OA, this metabolic adaptation and the self-repair ability of cartilage decrease and result in severe tissue damage and new bone formation[17,18]. Cartilage is an avascular tissue, and the nutrients that maintain the regular physiological activity are mostly infiltrated through the joint fluid and dispersed through the matrix to nourish the CHs. CHs generate ATP for energy metabolism, primarily dependent on glucose uptake and glycolytic metabolism. Once the energy metabolism balance of CHs is broken, ATP generation is profoundly decreased, which seriously affects the normal function of articular cartilage, and CHs are forced to degenerate.

In this study, we verified that the CHs of OA cartilage utilized less glucose and generated less ATP compared to the normal CHs, which was confirmed by the IL-1β induced CHs degeneration

in vitro. As the CHs generate the majority (>60%) of their ATP through glycolysis, the disorder of glucose uptake is responsible for the loss of ATP accumulation[19]. Accompanying with the imbalanced energy metabolism, we found the HIF-1α and Runx2 expression were upregulated under both the natural and IL-1β caused states. HIF-1α gene is the primary regulator of cells adapting to hypoxia stimulation. HIF-1α is mainly regulated by extracellular oxygen concentration. When the cell is under normoxia condition, HIF-1α can be degraded by ubiquitination. When the cell is in a hypoxic state, HIF-1α cannot be degraded and is overexpressed in the cell involving in energy metabolism, angiogenesis, and cytokines synthesis. In addition to oxygen partial pressure, Yudoh et al[13] also announced that metabolic disorders, IL-1β, and other inflammatory stimuli could induce the activation of HIF-1α in CHs. CHs lacking the HIF-1α gene cannot produce energy and synthesize substrates under both normal and hypoxic conditions, which accelerates the metabolic stress-induced apoptosis.

In addition to hypoxic factors, the metal ions Co^{2+} and Ni^{2+} are reported to stabilize HIF-1α activity and induce the expression of downstream genes by the replacement of Fe^{2+} to reduce HIF-1α degradation[20,21]. Different stimulation regulates the expression of HIF-1α through distinct signaling pathways, including interleukin 1 (IL-1)[22], tumor necrosis factor (TNF)[23], fibroblast growth factor (FGF)[24], p38/extracellular signal-regulated kinase (ERK)[25], and mitogen-activated protein kinase (MAPK)[26] pathways. However, the exact molecular mechanism that triggering the activation of HIF-1α in CHs remains unclear. Runx2 is an essential transcriptional regulator of bone formation and CH maturation. It transcriptionally upregulates various mineralization-related protein genes in pre-osteoblasts and CHs to differentiate the corresponding direction of osteogenesis. Runx2 is weakly expressed in dormant and proliferating CH, but it is upregulated in hypertrophic and terminal hypertrophic conditions, which plays a vital role in the process of cartilage degeneration[27]. Therefore, we wondered whether the upregulation of Runx2 induced the activation of HIF-1α. By silencing the Runx2 expression, the CHs hypertrophic genes, such as Col-I, Col-X, and MMP13, were suppressed under the stimulation of IL-1β. The HIF-1α expression was also not increased. However, cellular glucose uptake and ATP generation were also further decreased. These findings suggested that Runx2 silencing failed to raise the upregulation of HIF-1α, resulting in the profound reduction of glycolytic metabolism. Similarly, the silencing of HIF-α did not significantly affect the hypertrophic progression of CHs, but it aggravated the glycolytic metabolism under the IL-1β treatment. Besides, blocking HIF-1α did not impact Runx2 expression. Compared to the control, it was clear that HIF-1α and Runx2 were upregulated during CHs degeneration. If HIF-1α or Runx2 expression was not upregulated, the glycolytic metabolism would get further worse. Therefore, the upregulation of HIF-1α contributes to the self-repair of glycolytic metabolism. Consequently, we hypothesized that the activation of Runx2 triggers the HIF-1α upregulation, which contributes to the repair of glycolytic metabolism.

During endochondral bone formation, Lee et al[28] elucidated that Runx2 protein stabilizes HIF-1α in the hypertrophic CHs of the growth plate. But they did not mention Runx2 plays a role in the activation of HIF-1α. Fortunately, we found seven predicted sites in which Runx2 binds to the first 2000 sequences of HIF-1α promoter. After verification, we found there were at least two binding sites that Runx2 protein binds to the HIF-1α promoter regions. Furthermore, the 'aacgtcaaa' sequence of HIF-1α was significantly activated by the presence of Runx2 protein, which sufficiently proved that Runx2 could induce HIF-1α expression at the transcriptional level.

Conclusions

Glucose plays a vital role in the development, stabilization, repair, and remodeling of cartilage. Disturbance of glycolytic metabolism will damage cartilage tissue and CH functions. The novelty of our work is to clarify the increased HIF-1α expression in the degenerative CH is regulated by the Runx2 protein, which helps us to understand the mechanism of self-repair of glycolytic metabolism. However, Runx2 is also a negative factor in the progress of CH degeneration. In the OA process, whether Runx2 can be used to regulate HIF-1α expression without accelerating the process of CH degeneration remains to be further investigated.

Conflict of Interests

The authors declare that they have no conflict of interest.

References

1) Scanzello CR. Role of low-grade inflammation in osteoarthritis. Curr Opin Rheumatol 2017; 29: 79-85.
2) Loftus RM, Finlay DK. Immunometabolism: cellular metabolism turns immune regulator. J Biol Chem 2016; 291: 1-10.
3) Michalek RD, Rathmell JC. The metabolic life and times of a T-cell. Immunol Rev 2010; 236: 190-202.
4) Gomez R, Lago F, Gomez-Reino J, Dieguez C, Gualillo O. Adipokines in the skeleton: influence on cartilage function and joint degenerative diseases. J Mol Endocrinol 2009; 43: 11-18.
5) Mobasheri A, Bondy CA, Moley K, Mendes AF, Rosa SC, Richardson SM, Hoyland JA, Bar-rett-Jolley R, Shakibaei M. Facilitative glucose transporters in articular chondrocytes. Expression, distribution and functional regulation of GLUT isoforms by hypoxia, hypoxia mimetics, growth factors and proinflammatory cytokines. Adv Anat Embryol Cell Biol 2008; 200: 1, 1-84.
6) Loeser RF, Collins JA, Diekman BO. Ageing and the pathogenesis of osteoarthritis. Nat Rev Rheumatol 2016; 12: 412-420.
7) Mobasheri A. Glucose: an energy currency and structural precursor in articular cartilage and bone with emerging roles as an extracellular signaling molecule and metabolic regulator. Front Endocrinol (Lausanne) 2012; 3: 153.
8) Shikhman AR, Brinson DC, Valbracht J, Lotz MK. Cytokine regulation of facilitated glucose transport in human articular chondrocytes. J Immunol 2001; 167: 7001-7008.
9) Gavriilidis C, Miwa S, von Zglinicki T, Taylor RW, Young DA. Mitochondrial dysfunction in osteoarthritis is associated with down-regulation of superoxide dismutase 2. Arthritis Rheum 2013; 65: 378-387.
10) Toh WS, Brittberg M, Farr J, Foldager CB, Gomoll AH, Hui JH, Richardson JB, Roberts S, Spector M. Cellular senescence in aging and osteoarthritis. Acta Orthop 2016; 87: 6-14.
11) Ramakrishnan P, Hecht BA, Pedersen DR, Lavery MR, Maynard J, Buckwalter JA, Martin JA. Oxidant conditioning protects cartilage from mechanically induced damage. J Orthop Res 2010; 28: 914-920.
12) Schipani E, Ryan HE, Didrickson S, Kobayashi T, Knight M, Johnson RS. Hypoxia in cartilage: HIF-1alpha is essential for chondrocyte growth arrest and survival. Genes Dev 2001; 15: 2865-2876.
13) Yudoh K, Nakamura H, Masuko-Hongo K, Kato T, Nishioka K. Catabolic stress induces expres-sion of hypoxia-inducible factor (HIF)-1 alpha in articular chondrocytes: involvement of HIF-1 alpha in the pathogenesis of osteoarthritis. Arthritis Res Ther 2005; 7: R904-R914.
14) Komori T. Runx2, an inducer of osteoblast and chondrocyte differentiation. Histochem Cell Biol 2018; 149: 313-323.
15) Catheline SE, Hoak D, Chang M, Ketz JP, Hilton MJ, Zuscik MJ, Jonason JH. Chondrocyte-specific RUNX2 overexpression accelerates post-traumatic osteoarthritis progression in adult mice. J Bone Miner Res 2019; 34: 1676-1689.
16) Makris EA, Gomoll AH, Malizos KN, Hu JC, Athanasiou KA. Repair and tissue engineering techniques for articular cartilage. Nat Rev Rheumatol 2015; 11: 21-34.
17) Hunter DJ, Bierma-Zeinstra S. Osteoarthritis. Lancet 2019; 393: 1745-1759.
18) Guilak F, Nims RJ, Dicks A, Wu CL, Meulenbelt I. Osteoarthritis as a disease of the cartilage pe-ricellular matrix. Matrix Biol 2018; 71-72: 40-50.
19) Yang X, Chen W, Zhao X, Chen L, Li W, Ran J, Wu L. Pyruvate kinase M2 modulates the gly-colysis of chondrocyte and extracellular matrix in osteoarthritis. DNA Cell Biol 2018; 37: 271-277.
20) Kim J, So D, Shin HW, Chun YS, Park JW. HIF-1alpha upregulation due to depletion of the free ubiquitin pool. J Korean Med Sci 2015; 30: 1388-1395.
21) Epstein AC, Gleadle JM, McNeill LA, Hewitson KS, O'Rourke J, Mole DR, Mukherji M, Met-zen E, Wilson MI, Dhanda A, Tian YM, Masson N, Hamilton DL, Jaakkola P, Barstead R, Hodgkin J, Maxwell PH, Pugh CW, Schofield CJ, Ratcliffe PJ. C. elegans EGL-9 and mammali-an homologs define a family of dioxygenases that regulate HIF by prolyl hydroxylation. Cell 2001; 107: 43-54.
22) Wu S, Li H, Yu L, Wang N, Li X, Chen W. IL-1beta upregulates Muc5ac expression via NF-kappaB-induced HIF-1alpha in asthma. Immunol Lett 2017; 192: 20-26.
23) Kim KW, Lee SJ, Kim JC. TNF-alpha upregulates HIF-1alpha expression in pterygium fibro-blasts and enhances their susceptibility to VEGF independent of hypoxia. Exp Eye Res 2017; 164: 74-81.
24) Shi YH, Bingle L, Gong LH, Wang YX, Corke KP, Fang WG. Basic FGF augments hypoxia induced HIF-1-alpha expression and VEGF release in T47D breast cancer cells. Pathology 2007; 39: 396-400.
25) Jeong HJ, Hong SH, Park RK, Shin T, An NH, Kim HM. Hypoxia-induced IL-6 production is associated with activation of MAP kinase, HIF-1, and NF-kappaB on HEI-OC1 cells. Hear Res 2005; 207: 59-67.
26) Mi C, Ma J, Wang KS, Zuo HX, Wang Z, Li MY, Piao LX, Xu GH, Li X, Quan ZS, Jin X. Im-peratorin suppresses proliferation and angiogenesis of human colon cancer cell by targeting HIF-1alpha via the mTOR/p70S6K/4E-BP1 and MAPK pathways. J Ethnopharmacol 2017; 203: 27-38.
27) Liu CF, Samsa WE, Zhou G, Lefebvre V. Transcriptional control of chondrocyte specification and differentiation. Semin Cell Dev Biol 2017; 62: 34-49.
28) Lee SH, Che X, Jeong JH, Choi JY, Lee YJ, Lee YH, Bae SC, Lee YM. Runx2 protein stabiliz-es hypoxia-inducible factor-1alpha through competition with von Hippel-Lindau protein (pVHL) and stimulates angiogenesis in growth plate hypertrophic chondrocytes. J Biol Chem 2012; 287: 14760-14771.